

## High-Frequency Modes in a Two-Dimensional Rectangular Room with Windows

E. D. Shabalina<sup>a</sup>, N. V. Shirgina<sup>b</sup>, and A. V. Shanin<sup>b</sup>

*Institute of Technical Acoustics, Aachen University, Neustrasse 50, Aachen, 52066 Germany*

*Physics Faculty, Moscow State University, Moscow, 119992 Russia*

*e-mail: andrey\_shanin@mail.ru*

Received December 18, 2009

**Abstract**—We examine a two-dimensional model problem of architectural acoustics on sound propagation in a rectangular room with windows. It is supposed that the walls are ideally flat and hard; the windows absorb all energy that falls upon them. We search for the modes of such a room having minimal attenuation indices, which have the expressed structure of billiard trajectories. The main attenuation mechanism for such modes is diffraction at the edges of the windows. We construct estimates for the attenuation indices of the given modes based on the solution to the Weinstein problem. We formulate diffraction problems similar to the statement of the Weinstein problem that describe the attenuation of billiard modes in complex situations.

**DOI:** 10.1134/S1063771010040184

### INTRODUCTION

One of the fundamental problems in architectural acoustics is estimating the reverberation time of a room. The oldest and most popular approach is the Sabine formula [1], which is based on the supposition of a diffuse character of the sound field in the room. Clearly, the field assumes a diffuse character owing to the complex form of the room or diffuse reflection from wall coatings. In the present study, we examine the opposite case. We suppose that the walls are ideally flat and hard; the room geometry is chosen as rectangular. The only element making the problem nontrivial is the windows. In an exact formulation of the problem, we suppose that the walls are rigid borders of a certain rectangular area in an infinite space. The windows are obtained by removing certain areas of the boundary. An acoustic wave is diffracted on the windows, and its energy is carried away into open space. Such an exact formulation will be replaced below by a simplified one, which, however, does not qualitatively change the results. For simplicity, we consider a two-dimensional model problem.

Note that the case of a rectangular geometry and well-reflecting walls is not rare for architectural acoustics. This refers to all typical rooms without special partitioning. Windows can be apertures in the walls, as well as perfectly matching absorbing elements [2].

The described system is an open resonator. We search for the eigenmodes of this resonator, i.e., the expression for the field within the limits of the room, as well as for the resonance frequencies. We suppose that the field of each mode has a dependence on time in the form of  $\exp\{-i\omega_j t\}$ , where resonance frequency  $\omega_j$

is a complex quantity:  $\omega = \omega'_j - i\omega''_j$ . The imaginary part  $\omega''_j$  corresponds to mode attenuation.

We consider the high-frequency approximation; that is, we suppose that  $\omega' \gg c/L$ , where  $c$  is the speed of sound and  $L$  is the characteristic dimension of the room. We assign a sufficiently large actual value  $\omega_0$  and search for the mode with  $\omega' \approx \omega_0$ . As well, we are only interested in the mode with small values  $\omega''$ , i.e., modes with small attenuation.

We define the concept of small attenuation. Let the area occupied by the resonator (in the two-dimensional model, it plays the role of the room's volume) be equal to  $S$ ; the entire perimeter of the room, equal to  $P$ ; and the total length of the cutoffs/windows, equal to  $P'$ . Under the supposition of diffuse character of the field, the mean frequency of sound particle collision in the boundaries of the rectangle can be estimated as

$$\sigma \sim \frac{cP}{\pi S}.$$

The frequency of collisions with windows is

$$\sigma' \sim \frac{P' c P}{P \pi S} = \frac{c P'}{\pi S}. \quad (1)$$

The mean lifetime of a sound particle can be estimated as  $(\sigma')^{-1}$ ; this means that  $\sigma'$  is the estimate of the attenuation index when the field has a diffuse character. We are interested in modes that have

$$\omega'' \ll \sigma';$$

i.e., they have an attenuation index that is substantially less than the given estimate. Obviously, such modes

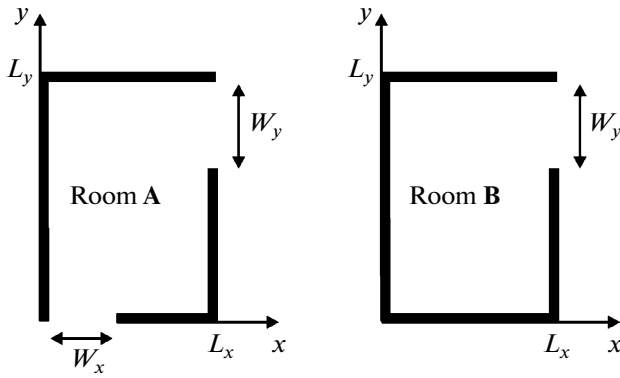


**Fig. 1.** Geometry of the studied resonators.

make the fundamental contribution to a steady-state field and to the reverberation process.

#### STATEMENT OF THE PROBLEM

In the given paper, we consider two rooms (room **A** and room **B**) the geometry of which is shown in Fig. 1. Room **A** has two windows, and room **B** has one window. Below we show that, owing to differing geometry, these rooms belong to different classes and the structure of their eigenmodes differs.

The dimensions of these two rooms are  $L_x \times L_y$ . The widths of the windows for room **A** are  $W_x$  and  $W_y$ . The width of the single window in room **B** is  $W_y$ . The walls of the room have a small but finite thickness (Fig. 2). On the walls, the Neumann boundary conditions are assigned. In the free space, the Helmholtz equation is fulfilled:

$$\Delta u + \frac{\omega^2}{c^2} u = 0.$$

It is necessary to include in the statement of the problem the condition of radiation at infinity and the Meixner conditions at corner points. These conditions have a standard form, and we do not give them here.

To numerically solve the problem, we use the boundary integral equation in the so-called direct formulation [3]. Namely, the Green's formula is used, which expresses the value of the field in the air and on the boundary by means of its value on the boundary in the following way:

$$c(r)u(r) = \int_{\Gamma + \Gamma_1} [G(r, r')\partial_n u(r') - u(r')\partial_n G(r, r')]dl', \quad (2)$$

where  $r$  is the radius vector of a point in the air or at the boundary;  $r' = r'(l)$  is the radius vector of a point on

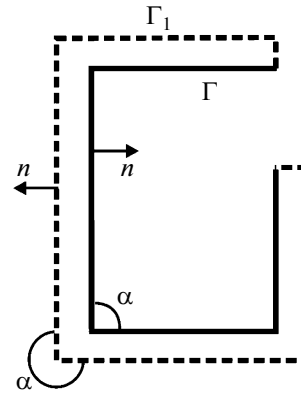


**Fig. 2.** Walls of the room (derivation of the boundary integral equation).

the boundary;  $G$  is the Green's function of an infinite plane,

$$G(r, r') = G(|r - r'|) = -\frac{i}{4}H_0^{(1)}(|r|\omega/c); \quad (3)$$

$c(r)$  is a coefficient with a value of 1 in air, 1/2 on smooth areas of the boundary, and  $\alpha/(2\pi)$  at corner points (see Fig. 2). Due to the boundary conditions, the first element under integral (2) is zero. Considering only points on the boundary, we obtain the boundary integral equation

$$2c(l)u(l) = \int_{\Gamma + \Gamma_1} K(l, l')u(l')dl', \quad (4)$$

$$K(l, l') = -2\partial_n G(|r(l) - r(l')|).$$

Note that the factor  $2c(l)$  is unequal to unity only at corner points. To simplify calculations, we make one more approximation. The boundary of the area occupied by the wall consists of two parts,  $\Gamma$  and  $\Gamma_1$ . In calculations the contribution to the integral relating to area  $\Gamma_1$  was neglected; that is, in Eq. (4), variables  $l$  and  $l'$  only ran through points related only to area  $\Gamma$ . This approximation is justified because the field on the external surface of the boundary is small everywhere with the exception of the edges of the window, where the diffraction field is generated. Here we ignore subtle details of the diffraction process. Note that diffraction is the main attenuation mechanism of the considered modes; however, Fresnel diffraction is of interest: wave scattering under angles close to that of mirror reflection. As well, the dimension of the zone near the edge of the scatter responsible for diffraction is approximately  $\sim \sqrt{L\lambda}$ ; that is, this is the dimension of the first Fresnel zone. Here,  $L$  is the characteristic dimension of the room and  $\lambda$  is the wavelength. Our approximation consists in ignoring a zone on the order of  $\lambda$  on the external side of the boundary. Comparing  $\sqrt{L\lambda}$  and  $\lambda$ , we arrive at the conclusion that the ignored contributions are not large. The given simplification, of course,

strongly influences the scattering of rays at large angles (it influences Keller diffraction), but has almost no effect on Fresnel diffraction.

Operator  $\tilde{K}$  depends on  $\omega$  as on a parameter. Our goal is to choose this parameter in such a way that unity belongs to the spectrum of the given operator. Discretization is performed using the method of boundary elements, the given operator is approximated as matrix  $\tilde{K}$ , and

$$\det(\tilde{K} - I) = 0 \quad (5)$$

becomes the criteria for solving Eq. (5).

If (5) is satisfied, then matrix  $\tilde{K} - 1$  has an eigenvector that represents a set of eigenmode values in the mesh nodes given on the internal surface of the boundary. The mode inside the room can then be restored according to be boundary values with the help of formula (2). It is precisely this scheme that we will follow in carrying out the numerical experiment.

### PRELIMINARY ANALYSIS: VIRTUAL RESONATORS

We will examine families of rays describing closed billiard trajectories in a rectangular room without windows (see Fig. 3). Each such trajectory is characterized by a pair of a mutually simple nonnegative integers  $(M, N)$ . As well, the angles at which the rays propagate along the  $x$  axis are

$$\alpha, -\alpha, \pi - \alpha, \pi + \alpha,$$

where

$$\tan \alpha = \frac{NL_y}{ML_x}.$$

It is easy to check that the length of each closed trajectory is

$$D_{M,N} = 2\sqrt{(ML_x)^2 + (NL_y)^2}.$$

We will call the pair of simple nonnegative whole numbers  $(M, N)$  in the resonator the *rational direction*.

We return to the room with windows. We consider a family of rays corresponding to rational direction  $(M, N)$ . Each ray is reflected from the walls several times. If at least one act of reflection occurs on the window, the ray loses its energy and cannot participate in generating a high-quality mode. We call this a *disappearing ray*. If only disappearing rays correspond to a certain rational direction, we also say that this direction is *disappearing*. On the other hand, if nondisappearing rays correspond to a certain rational direction, we call this direction *nondisappearing*. In this way, all rational directions are divided into two classes.

Families of rays (that is, beams) that generate billiard trajectories correspond to nondisappearing directions. High-frequency waveguide modes corre-

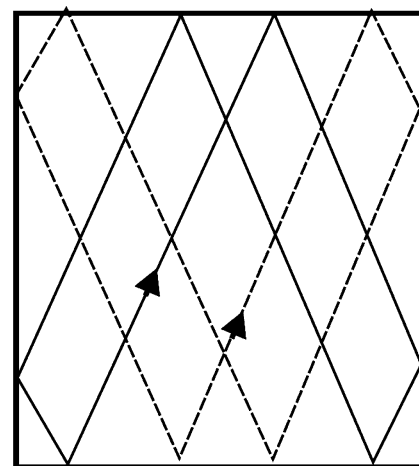


**Fig. 3.** Billiard trajectories in a room without windows.

spond to these families. Consequently, every nondisappearing direction represents a virtual resonator, the mode structure in which we will study below. Such an approach corresponds to the concept of a multimirror resonator [4].

The room can have a finite or infinite number of nondisappearing rational directions. The main difference between rooms **A** and **B**, depicted in Fig. 1, is precisely that room **A** has a finite number and room **B** has an infinite number of such directions. If  $W_x > L_x/3$  and  $W_y > L_y/3$ , for room **A**, only the directions

$$(0,1), (1,0), (1,1)$$

are nondisappearing.

As well, if  $W_y > L_y/2$ , then for room **B**, the directions

$$(0,1), (n,1), \quad n = 0, 1, 2\dots$$

are nondisappearing.

If there is an infinite number of nondisappearing rational directions, then there exists a limit point, that is, a direction (in our case necessarily rational) in any neighborhood of which there is an unlimited number of nondisappearing directions. Below we show that the existence of a limit point complicates the mode structure in the room.

### FABRY-PEROT-TYPE MODES

We clarify the mode structure, which represents a set of nondisappearing billiard trajectories in a virtual resonator. We fix the nondisappearing direction. Let for simplicity the direction be not parallel to the walls; i.e.,  $M \neq 0$  and  $N \neq 0$ . For the given family of rays we apply the reflection method. We reflect the room relative to its walls and do the same with the obtained reflections, etc. We suppose that the walls are ideally hard; therefore, we can consider that a ray does not see the walls and crosses into the next-in-turn "world

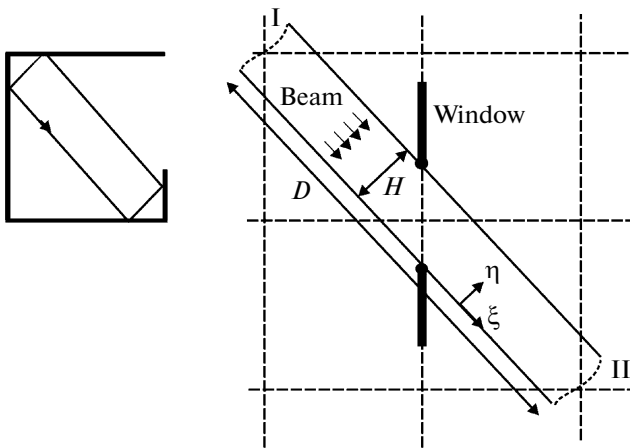


**Fig. 4.** Application of the reflection method to a nondisappearing family of rays.

beyond the mirror" without distortion. As well, as it hits a window (or their reflections), the ray is fully absorbed. In this way, there are no walls in the constructed system of reflections and the windows are ideally absorbing screens (see Fig. 4).

As a result of using the reflection method, each virtual resonator described in the preceding section becomes a waveguide like an aperture line. As well, the beam crossing through the aperture line should satisfy the periodicity condition. Namely, the field in cross sections along length  $D$ , determined like (10), should be identical (in Fig. 3, these are cross sections I and II). We will suppose that the beam width, determined by the geometry of the aperture line, is  $H$ .

The problem of the aperture-line-type waveguide arises naturally in studying the classic problem of modes in a Fabry–Perot resonator. Let there be a two-dimensional acoustic resonator consisting of two ideally hard plane-parallel mirrors of width  $H$ . Let the

distance between the mirrors be  $D/2$  (see Fig. 5). We apply the reflection method to the given problem. As a result, the resonator becomes an aperture-line-type waveguide. For the field in such a waveguide to correspond to the field in the initial resonator, it is necessary that it satisfy the periodicity condition at length  $D$ .

Logically, in the given statement of the problem, extensions of the mirrors cannot be replaced by ideally absorbing screens. As well, it is necessary to take into consideration the structure of the edges of the mirrors. However, it is known that in the case of short waves, as well as of predominantly normal (relative to the mirrors) propagation of the beam, the field in the resonator is well described by the parabolic equation [5, 6, 7]. For instance, such an approach is equivalent to the classical Fox–Lee integral equation. In writing such integral equations, we simply ignore the field at extensions of the mirrors, which corresponds to ideally absorbing screens.

The aperture line depicted in Fig. 5, in the general case, differs from aperture lines obtained from virtual resonators. The following features are characteristic of it:

- it has exactly two pairs of absorbing screens per period;
- screens on different sides of the beam are situated on a straight line;
- the screens are situated along the normal to the beam axis.

In analyzing virtual resonators, aperture lines are obtained that can have a different number of screens from different sides of the beam. In addition, they do not have to be situated along the normal to the axis. To obtain estimates, we simplify the task, considering screens to be located along the normal to the axis of the waveguide and retaining the position of the edges of the screens (see Fig. 6). Note that diffraction on a system of inclined (reflecting, but not absorbing)

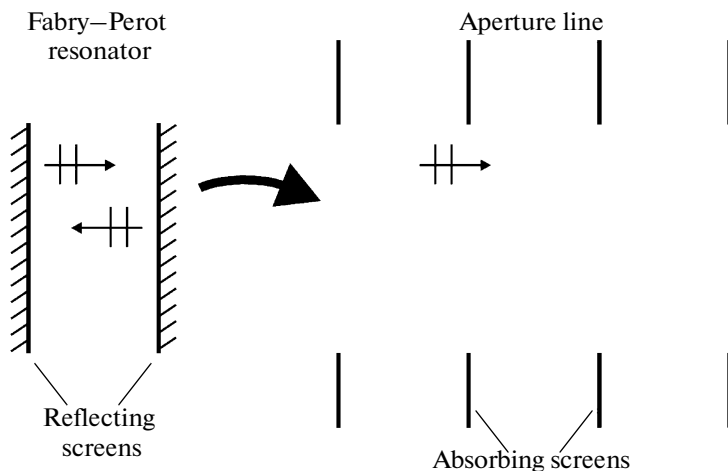


**Fig. 5.** Aperture line for a Fabry–Perot resonator.

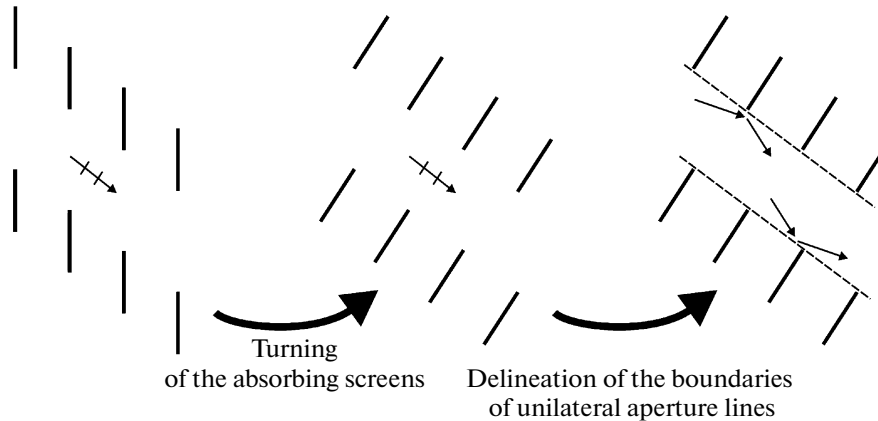


**Fig. 6.** Continuous simplification of the problem on the aperture line for a virtual resonator.

screens was studied in [8]. Further simplification consists in studying systems of screens on different sides of the beam independently of each other. As well, we calculate the coefficient of reflection of a plane wave falling at a small angle from a unilateral aperture line. Scattering into higher modes is ignored (the respective coefficients are small), and it is possible to consider that there is a plane wave undergoing reflection from two boundaries of unilateral aperture lines. These boundaries have a reflection coefficient close to  $-1$ . The exact value of the reflection coefficient for a line with periodically situated screens is determined by the method developed by L.A. Weinstein [5]. Corrections to the reflection coefficient make it possible to estimate the quality of modes in virtual resonators.

The condition where scattering on two systems of screens can be considered independently reduces to the dimension of the first Fresnel zone being much smaller than the beam width:  $\sqrt{D/k_0} \ll H$ . This is equivalent to condition (8) for the first of the modes examined below.

Thus, we apply the Weinstein method if (a) with every side of the resonator the screens are situated at equal distances along the axis (these periods are probably different to the right and left of the beam); (b) the angle between the normal to the surface of the windows and the beam axis is not close to  $\pi/2$  (that is, the absorbing screens are not parallel to the axis of the aperture line); (c) the inequality  $\sqrt{D/k_0} \ll H$  is satisfied. If condition (a) or (b) is not met, it is necessary to solve one of the new diffraction problems formulated below.

We introduce coordinate  $\xi$  along the beam and coordinate  $\eta$  across the beam. We will consider sets  $\eta = 0$  and  $\eta = H$ . We will search for the field in the form of

$$u = a \exp \{i(k_\xi \xi + k_\eta \eta)\} + b \exp \{i(k_\xi \xi - k_\eta \eta)\}, \quad (6)$$

i.e., in the form of the sum of two plane waves. We introduce the angle

$$\sin \theta = \frac{k_\eta}{\sqrt{k_\xi^2 + k_\eta^2}}. \quad (7)$$

This is the angle between the direction of propagation of the plane waves and the beam axis. The given angle should be small. It is known that the condition of applicability of the waveguide approach is

$$\beta \ll 1, \quad (8)$$

$$\beta = \theta \sqrt{k_0 D}, \quad (9)$$

where  $k_0 = \omega_0/c$  (see [5] and [9]).

The key result of the Weinstein theory for our case is as follows. In satisfying conditions  $k_0 D \gg 1$ ,  $k_0 H \gg 1$  and (8), it is possible to consider that plane waves (6) are reflected from the boundaries of the aperture line almost like from the boundary with the Dirichlet condition, i.e.,

$$a = R_1 b, \quad b = R_2 a \exp \{2ik_\eta H\},$$

with  $R_1 \approx -1$  and  $R_2 \approx -1$ . The given result is nontrivial, and there is no simple explanation for it. Technically, Weinstein obtained it as a result of solving the problem of radiation from the open end of a plane waveguide. He used the Wiener–Hopf method [10].

Reflection coefficients  $R_1$ ,  $R_2$  differ from  $-1$  in the first order of  $\beta$ . Corrections to the reflection coefficients determine the mode attenuation in the aperture line and, in the final analysis, make it possible to calculate the attenuation index of the corresponding mode in a virtual resonator.

Before anything else, we determine the structure of modes on the given aperture line. Neglecting corrections to reflection coefficients, we find that the modes have a transversal structure characteristic of a resonator with a soft boundary:

$$u(\xi, \eta) = \sin(\pi j \eta / H) \exp \{ik_\xi \xi\}, \quad (10)$$

where  $j = 1, 2, 3, \dots$  is the transversal index of the mode. In this way,

$$k_\eta \approx \frac{\pi j}{H}. \quad (11)$$

The longitudinal wave number is determined from the periodicity condition:

$$\exp\{ik_\xi D\} = 1, \quad (12)$$

i.e.,

$$k_\xi = \frac{2\pi r}{D}, \quad (13)$$

where  $r = 0, 1, 2, \dots$  is the longitudinal mode index. Thus, each Fabry–Perot-type mode in the room is defined by the rational direction (i.e., by the virtual resonator to which this mode belongs), the transversal index  $j$ , and longitudinal index  $r$ . Virtual resonators with a large  $H$  correspond to high-quality modes. In addition, high-quality modes correspond to small values of index  $j$  and large values of index  $r$ .

Note that equality (13) is exact, since the periodicity condition does not depend on the properties of the aperture line, but equality (11) is approximate. Corrections to the reflection coefficients lead to the appearance of a negative imaginary addition in  $k_\xi$ . The value of  $k_\eta$  is determined from the relationship

$$R_1 R_2 \exp\{2ik_\eta H\} = 1, \quad (14)$$

which gives

$$k_\eta = \frac{\pi j}{H} - \frac{\ln(-R_1) + \ln(-R_2)}{2iH}.$$

Taking into account that  $k_\xi^2 + k_\eta^2 = \omega^2/c^2$  and  $k_\xi \gg |k_\eta|$ , we obtain the final formula for the mode attenuation index:

$$\omega'' \approx \frac{\pi j c^2}{2H^2 \omega} \operatorname{Re}[\ln(-R_1) + \ln(-R_2)]. \quad (15)$$

Note that consideration of the imaginary part in (15) makes it possible to find the small diffraction correction to the eigenmode frequency; however, this question is of no practical interest.

It is difficult to calculate  $\ln(-R_{1,2})$ . We can perform these calculations in a singular case, when ideally absorbing screens are situated at identical distances along the aperture line. In this case (see [5])

$$\ln(-R) \approx -\frac{0.824(1-i)\sqrt{dk_\eta}}{\sqrt{k_\xi}}, \quad (16)$$

where  $d$  is the period at which screens appear along axis  $\xi$ . The most typical cases include  $d = D$  (as shown in Fig. 4) and  $d = D/2$ .

In order to consider the remaining cases of interest (they are listed below), it is necessary to solve the cor-

responding very complex diffraction problem. Unfortunately, at present, solutions to these problems are unknown.

We will now summarize the results of this section. To each virtual resonator at sufficiently high frequencies there corresponds a family of modes indexed by two parameters: longitudinal index  $r$  and transversal index  $j$ . The mode represents a narrow beam of waves continuously reflected from the walls and having a closed trajectory. The beam structure is close to (10). The longitudinal wave number is determined from periodicity condition (12), and the transversal wave number, from condition (14). The mode attenuation index is calculated by formulas (15), (16). The condition of validity of (15) is inequality (8).

Note that in accordance with (11), it is possible to rewrite condition (8) in a form that includes only the parameters of the virtual resonator:

$$\frac{\pi j^2 c D}{H^2 \omega} \ll 1. \quad (17)$$

When  $j = 1$ , it is possible to interpret condition (17) from the viewpoint of elementary diffraction theory. Namely, it is possible to rewrite it in the form  $\sqrt{D\lambda} \ll H$ , which means that each scatterer of the aperture line is located in the near zone of the preceding diffuser.

## NUMERICAL EXPERIMENT

In this section, we numerically check the estimates made in the preceding section. We do this in the following way. We examine integral equation (3) with a kernel depending on  $\omega$ . We solve the problem of searching for complex values  $\omega$  lying near a certain fixed  $\omega_0$ ; that these values Eq. (3) has a nontrivial solution. Equation (3) is discretized, after which the condition of the existence of a nontrivial vector of solutions is written in matrix form (5). This relationship represents an (transcendental) equation relative to parameter  $\omega$ . The given equation is solved by iteration. For the current value  $\omega$ , we calculate the eigenvalue of the matrix  $\tilde{K}$  closest to 1; we calculate the correction to  $\omega$  by its deviation from unity, after which we repeat the process until the required accuracy is achieved. Afterwards, we calculate the eigenvector corresponding to a single eigenvalue and with the help of the Green's formula, the field in the room is restored.

We discretize Eq. 3 in the following way. Boundary  $\Gamma$  is divided into small areas (boundary elements) at each of which a node is chosen. On the boundary elements, an unknown function is approximated over the node values as a piecewise-constant function. After this, we write Eq. (3) relative to the nodes.

In the discretization of Eq. (3), we take into account the fact that the field may possess peculiarities near corner- and endpoints. As well, in our case, the field at corner points is regular and at endpoints it can

**Table 1.** Results of numerical experiment for room A

$(M, N)$	$j$	$\beta$	$k'', \text{m}^{-1}$	$H, \text{m}$	$d_1, \text{m}$	$d_2, \text{m}$	$k'', \text{m}^{-1} \text{ theor.}$
(1, 0)	1	0.5	0.004	2	3	6	0.0038
	2	1.0	0.013				0.0155
	3	1.5	0.028				0.0356
	4	2.0	0.053				0.0658
(1, 1)	1	0.6	0.005	2	11.6	11.6	0.006
	2	1.3	0.024				0.024
	3	1.9	0.049				0.057
(0, 1)	1	1.3	0.018	1	5	10	0.033

have a radical singularity. In order to retain accuracy in calculations, we apply a standard method: densening of the mesh close to corner- and endpoints. Along with the correct description of the features of the field, this method makes it possible, without substantial loss in accuracy, to suppose a coefficient  $2c$  everywhere equal to unity.

In this section, for convenience, we used a wave number of  $k = \omega/c$  instead of circular frequency  $\omega$ . Correspondingly, the initial value of the wave number is  $k_0$ , and its real and imaginary parts are designated  $k'$  and  $-k''$ .

The rational direction is designated with the help of indices  $M$  and  $N$  introduced earlier; i.e., each Fabry–Perot-like mode is designated by a group of four whole numbers including the direction, the transversal index, and the longitudinal index. As a result of solving the posed problem, for each rational direction and transversal index, it is possible to find a family of modes with longitudinal indices close to  $r = Dk_0/(2\pi)$ . All of these modes have very close attenuation indices and a similar field distribution. Therefore, from each such family we retain only one representative and do not show the longitudinal index.

Table 1 shows the results for room A. The following parameters were chosen for the calculations:

$$\begin{aligned} L_x &= 3 \text{ m}, & L_y &= 5 \text{ m}, & k_0 &= 62 \text{ m}^{-1}, \\ W_x &= 2 \text{ m}, & W_y &= 3 \text{ m}. \end{aligned}$$

The choice of  $k_0$  corresponds to a wavelength of 0.1 m and is determined by our computing capabilities. Recall that the iteration procedure requires multiple construction of matrix  $\tilde{K}$  and calculation of its eigen-numbers.

The constructed modes can easily be visually classified. The results of this classification are shown in the table. The first column is the rational direction to which the mode refers. The second column is the transversal index. The third column is the estimate

of parameter  $\beta$  by formula (9). The fourth column is the main result of the numerical experiment. This is the imaginary part of the wave number connected with the attenuation index of the mode by the formula  $\omega'' = k''c$ .

The fifth through eighth columns refer to theoretical estimates. Parameters  $H$ ,  $d_1$ , and  $d_2$  are the beam aperture and the periods of screens following on the boundaries of the beam. They are determined from the room geometry. The eighth parameter is the estimate  $k''$  by formula (15). Taking into account that parameter  $\beta$  does not anywhere dip sufficiently low, correspondence between estimates and numerical results can be considered satisfactory. Note that only direction (1,1) refers to the type that can be calculated with the Weinstein theory. The beams of the remaining two directions propagate partially along the screens located at the boundary of the beams. Exact determination of the attenuation indices of these modes requires the solution of a new diffraction problem.

An important parameter of room A is estimate  $k''$  made under the supposition of diffuse field (1):

$$k''_{\text{diff}} = c\sigma' = \frac{P'}{\pi S'}$$

In our case,  $k''_{\text{diff}} \sim 0.1 \text{ m}^{-1}$ . Clearly, many of the modes obtained as a result of numerical experiment have quite a high quality in comparison to this estimate.

Figures 7 and 8 depict the character of the field in the eigenmodes. The given distributions have been obtained as a result of restoring the mode by the Green's formula. The figures are a contour representation of a two-dimensional function—the squared value of the field; these representations were done at a level of 0.1 of the maximal value.

The numerical experiment for room B was conducted with the following parameter values:

$$L_x = 3 \text{ m}, \quad L_y = 5 \text{ m}, \quad k_0 = 62 \text{ m}^{-1}, \quad W_y = 3 \text{ m}.$$

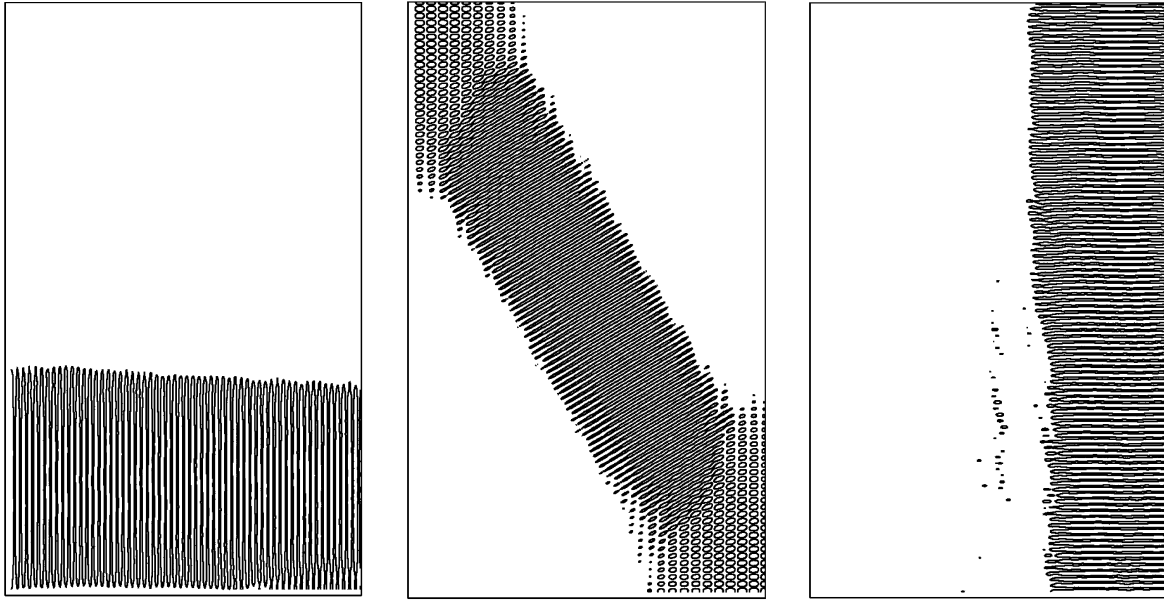


**Fig. 7.** Modes of room A. Directions  $(1,0)$ ,  $(1,1)$ ,  $(0,1)$ ; transversal index  $j = 1$ .

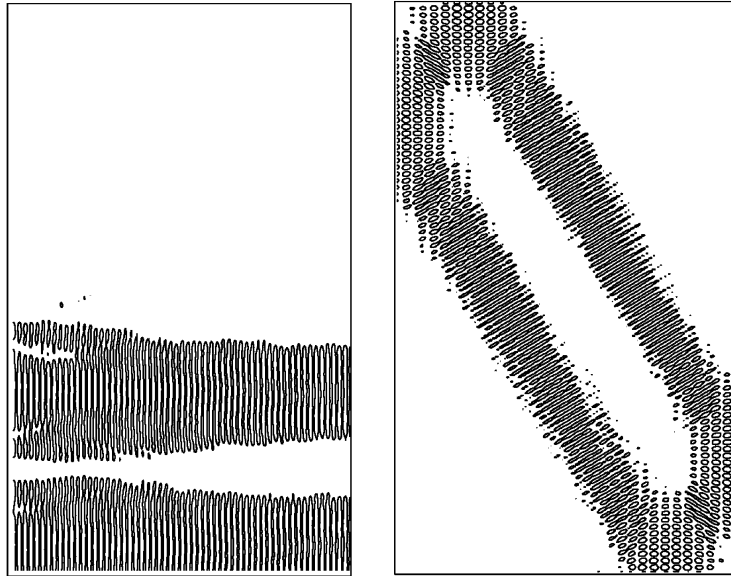


**Fig. 8.** Modes of room A. Directions  $(1,0)$ ,  $(1,1)$ , transversal index  $j = 2$ .

Part of the modes were classified as Fabry–Perot modes. The data on these modes are given in Table 2. The geometry of virtual resonators  $(1,1)$  and  $(1,2)$  corresponds to the aperture line examined above. The geometry of resonator  $(1,1)$  also corresponds to the aperture line if we consider it together with a geometrical reflection in the wall of  $y = 0$ . Because of this it makes sense to examine only the odd (symmetrical) modes in such a resonator. We consider virtual resonator  $(0,1)$  along with its reflection in the wall of  $x = 0$ ,

but its geometry is more complex. At the beam boundary  $x = L_x$  parallel to the beam axis, there is a wall. Such a beam is not described by formula (15) (although, as the numerical experiment shows, this formula gives a fairly good estimate of attenuation). Certain modes of room **B**, listed in Table 2, are shown in Fig. 9.

In contrast to room **A**, where the numerical experiment showed only Fabry–Perot-type modes, room **B** has more complex modes. Some of these are shown in

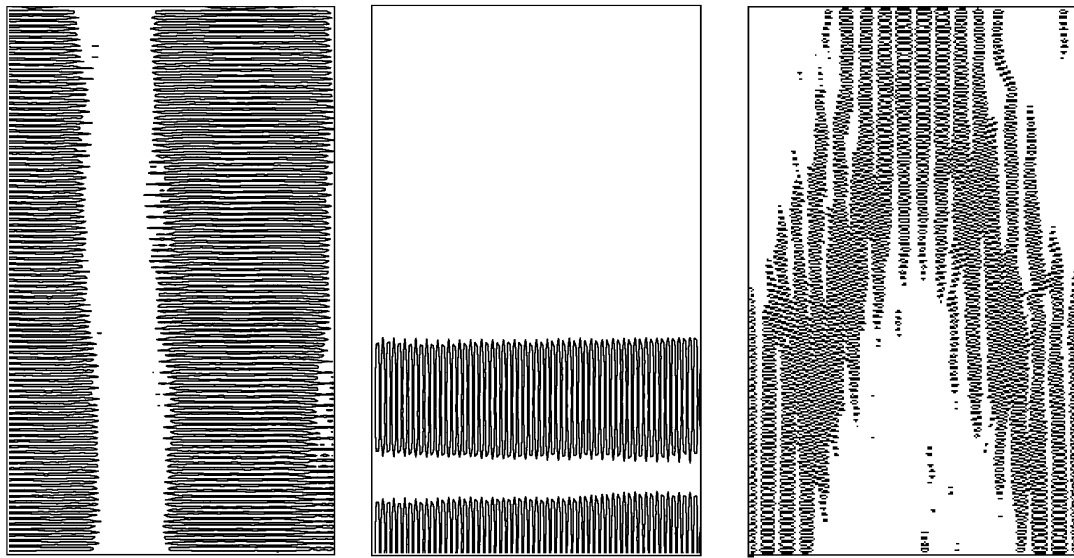


**Fig. 9.** Modes  $(0,1), j = 3; (1,0), j = 3; (1,2), j = 1$ .

Fig. 10. These modes have attenuation indices that are significantly lower than the diffusion estimate  $k'' \sim 0.05 \text{ m}^{-1}$ . Values  $k''$  for the given modes are shown in Table 3.

The given modes have the following interpretation. Each of them represents the sum of several Fabry–Perot modes for which condition (13) is essentially not met. In this case, the beam is scattered and there is an outflow of energy to different Fabry–Perot modes. If it turns out that these modes are synchronized according to frequency, a very-high-quality mixed mode is generated. In other words, such mixed modes are the result of interaction between Fabry–Perot modes.

Note that for Fabry–Perot modes to interact effectively, these modes should correspond to close rational directions. If the number of nondisappearing directions is finite, then with increasing frequency all these directions are far from one another; i.e., for the lowest modes in terms of the transversal index in these directions, condition (7) is met and there is no scattering into other modes. In contrast, when there is a limit point among the nondisappearing directions, near this point there will be interacting modes at any high frequency. In this way, the presence of high-quality mixed modes at high frequencies is a property of rooms with an infinite number of nondisappearing directions.

**Table 2.** Results of numerical experiment for room B: Fabry–Perot modes

$(M, N)$	$j$	$\beta$	$k'', \text{m}^{-1}$	$H, \text{m}$	$d_1, \text{m}$	$d_2, \text{m}$	$k'', \text{m}^{-1} \text{ theor.}$
$(1, 0)$	1	0.5	0.0004	4	6	6	0.00058
	3	1.0	0.0045				0.0053
	5	1.5	0.013				0.015
$(1, 1)$	1	0.6	0.0036	2	11.6	11.6	0.006
	2	1.3	0.014				0.024
	3	2.0	0.032				0.057
$(1, 2)$	1	1.5	0.014	1.7	20.9	20.9	0.018
$(0, 1)$	1	0.1	0.00025				0.00016
	3	0.4	0.0020	6	5	5	0.0014
	5	0.8	0.0032				0.004
	9	1.3	0.011				0.013
	13	1.9	0.018				0.030
	17	2.5	0.019				0.053

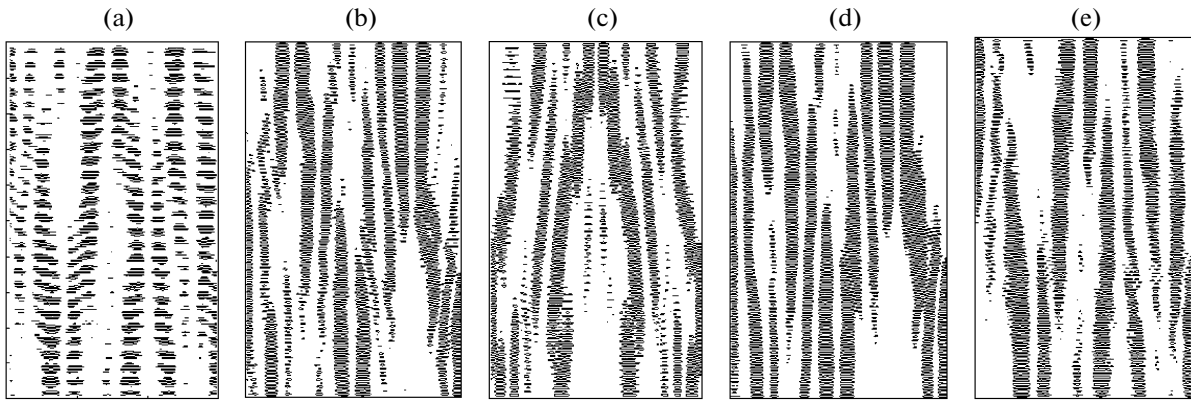


Fig. 10. Mixed modes of room B.

### ELEMENTARY ESTIMATE OF THE INDEX OF ATTENUATION OF MIXED MODES

Explaining the structure of mixed modes represents a separate relatively complex problem. Here we show that for room **B** there exists a combined mode and the attenuation index drops with an increase in frequency. The constructed estimate is very rough.

We select the frequency in such a way that the relationship

$$L_y \frac{\omega'}{c} = \pi J$$

is fulfilled for a certain large integer  $J$ . As well, the ray traveling along the  $y$  axis from one wall to the other and back returns with the same phase with which it left.

We apply the reflection method to room **B**. As a result, we obtain the two-dimensional periodic system of screens shown in Fig. 11. The periods of the structure are  $2L_x$  and  $2L_y$ , and all screens are parallel to the  $y$  axis and have length  $2W_y$ . The value of each aperture is  $2(L_y - W_y)$ . Beams traveling at small angles to the  $y$  axis correspond to mixed modes.

We use the periodicity of the system along the  $x$  axis and examine the passage of the wave from cross section  $x = L_x$  to cross section  $x = -L_x$ ; i.e., we look at one period of the system. Let in cross section  $x = L_x$ , from the side of positive  $x$ , a plane wave fall at a glancing angle to the apertures. Our task will be to estimate the value of the wave in the apertures in cross section  $x = -L_x$ .

Propagation occurs along the rays, one of which is shown in Fig. 11. The ray with index  $n$  connects point  $(L_x, y)$  with point  $(-L_x, y + 2nL_y)$ . This rate is charac-

terized by length  $R_n$  and angle  $\varphi_n$ . Clearly,  $\sin\varphi_n = 2L_x/R_n$ .

In accordance with the Green's formula, it is possible to estimate the partial amplitude corresponding to the ray with index  $n$  as

$$u_n = ik' \sin(\varphi_n)(L_y - W_y)G(kR_n), \quad (18)$$

where  $G(kR)$  is the plane Green's function:

$$\begin{aligned} G(kR_n) &= -\frac{e^{i\pi/4}}{4\sqrt{2\pi kR_n}} \exp\{ikR_n\} \\ &\approx -\frac{e^{i\pi/4}}{4\sqrt{2\pi k'R_n}} \exp\left\{ik'\frac{\varphi_n^2}{2}R_n + k''R_n\right\}. \end{aligned}$$

We will describe the exponential growth of all terms by the multiplier  $\exp\{k''R_{\text{eff}}\}$ , where  $R_{\text{eff}}$  will be estimated below. The field in the aperture can be estimated as the sum of contributions (18):

$$\begin{aligned} u &= -e^{i3\pi/4} \sqrt{\frac{k'}{2\pi}} L_x (L_y - W_y) \\ &\times \exp\{k''R_{\text{eff}}\} \sum_n R_n^{-3/2} \exp\left\{2i\frac{k'L_x^2}{R_n}\right\}. \end{aligned} \quad (19)$$

We estimate the sum entering into (19). Note that at large  $n$  the exponent is close to unity, but as  $n$  decreases, it begins to oscillate. The boundary of the oscillating behavior of the integral is obviously

$$R_{\text{eff}} \sim k'L_x^2,$$

and this is a good estimate (from below) for the effective length of the ray for calculating the exponentially growing multiplier in (19).

Table 3. Attenuation indices of mixed modes

Mode	a)	b)	c)	d)	e)
$k'', \text{m}^{-1}$	0.0076	0.009	0.0061	0.0060	0.0050

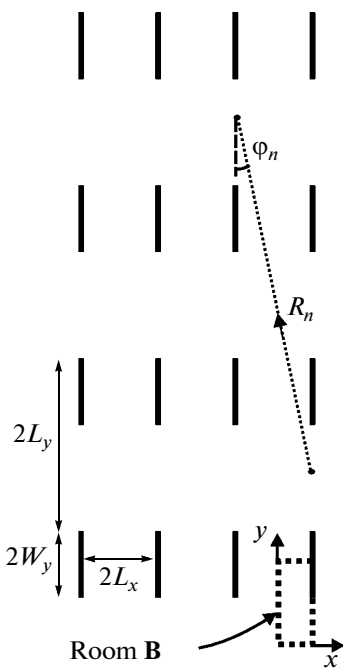


**Fig. 11.** Problem on propagation of creeping rays between apertures.

We replace the sum with the integral

$$\begin{aligned} & \sum_n R_n^{-3/2} \exp\left\{2i \frac{k' L_x^2}{R_n}\right\} \\ & \approx (2L_y)^{-3/2} \int_{v_0}^{\infty} v^{-3/2} \exp\left\{i k' \frac{L_x^2}{v L_y}\right\} dv, \end{aligned} \quad (20)$$

where the lower limit of integration  $v_0$  is chosen such that the exponent in (20) oscillates. The integral is eas-

ily calculated (its asymptotics do not depend on  $v_0$ ):

$$\sum_n R_n^{-3/2} \exp\left\{2i \frac{k' L_x^2}{R_n}\right\} \approx \sqrt{\frac{\pi i}{2k'}} \frac{1}{2L_x L_y}.$$

Finally,

$$u \approx \exp\{k'' R_{\text{eff}}\} \frac{L_y - W_y}{4L_y}.$$

From the condition on periodicity of the field in the aperture line,

$$k'' \sim \frac{1}{R_{\text{eff}}} \ln\left(\frac{4L_y}{L_y - W_y}\right) = \frac{1}{k' L_x^2} \ln\left(\frac{4L_y}{L_y - W_y}\right).$$

Thus, with increasing frequency (i.e., with increasing  $k'$ ), the quantity  $k''$  behaves as  $(k')^{-1}$ . This means that the index of attenuation of the given mode decreases. The corresponding estimate for any Fabry–Perot mode with fixed  $M$ ,  $N$ , and  $j$  is  $(k')^{-3/2}$ ; i.e., the index of attenuation of Fabry–Perot modes decreases more rapidly.

#### SOME DIFFRACTION PROBLEMS IMPORTANT FOR CALCULATING MODES IN RECTANGULAR ROOMS

As noted above, exact (in a high-quality approximation) description of Fabry–Perot modes is only possible in the case where at the boundary of the wave beam, the apertures form a system characteristic of the Weinstein problem. We take the Weinstein problem to mean a problem on the reflection of a high-frequency wave from a periodic system of ideally absorbing screens when there is grazing incidence. This problem is schematically depicted in Fig. 12a.

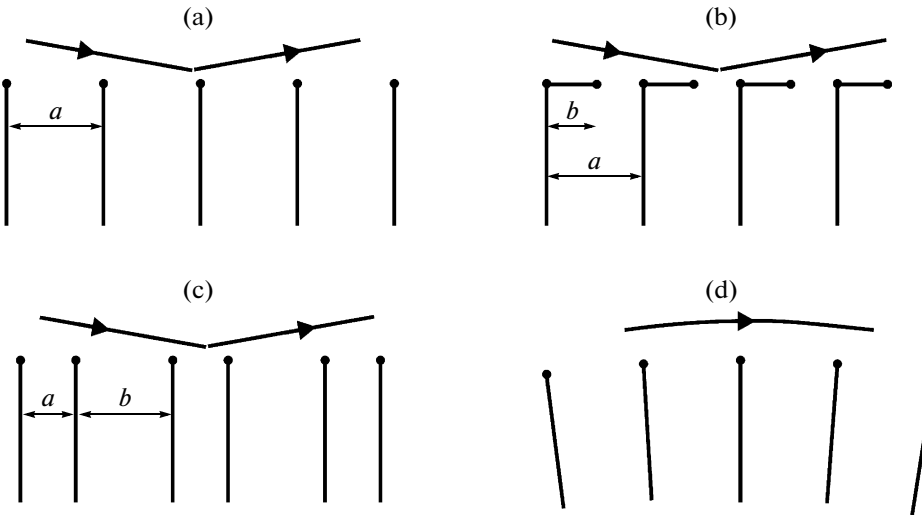


**Fig. 12.** Formulation of diffraction problems.

If the boundary of the beam passes along an area of a hard wall, it is necessary to solve the problem of reflection of a creeping wave from the structure shown in Fig. 12b. We suppose that horizontal scatters are hard, and vertical scatters, absorbing. This problem is very important, since this is the typical structure of the boundary for modes corresponding to the limit non-disappearing direction.

If the boundary of the beam passes near several edges of the windows, in order to describe such a mode, it is necessary to solve the problem of the type depicted in Fig. 12c.

Finally, if the walls in the room are not parallel but deviate at a small angle, it is necessary to solve the problem on propagation along a curved aperture line (Fig. 12d).

The authors know of no analytical solutions to problems b–d. It is possible that we can apply the Wiener–Hopf matrix method to problem c. We suppose that it may be possible to successfully apply the method put forth in [9] to the given problems.

Note that some complex problems on diffraction on periodic boundaries have been solved in [11–13].

## CONCLUSIONS

We have investigated the two-dimensional problem of high-frequency modes in a rectangular resonator with acoustically hard walls. It has windows that represent ideally absorbing fragments of walls.

We introduce the concept of a virtual resonator, which is a family of parallel closed billiard trajectories that do not hit the windows. The rooms are divided into two classes: those having a finite number of virtual resonators and those having an infinite number of virtual resonators.

For each virtual resonator in the case of a very simple boundary, we have examined the structure of modes and estimated the attenuation index of each mode. We have constructed an estimate on the basis of the Weinstein theory for the reflection of a wave in the aperture line. Each mode is characterized by the virtual resonator to which it belongs, the transversal index, and the longitudinal index.

We have conducted a numerical experiment for two rooms. Room A belongs to the first class (it has a finite number of virtual resonators), and room B belongs to the second class (it has an infinite number of resonators). We have shown that in the case of room A, we have found as a result of numerical experiment modes

that agree well with theoretical estimates. For room B, along with Fabry–Perot modes, we have found mixed modes, which are the sum of several Fabry–Perot modes lying close to the limit direction.

We have estimated the attenuation index for a mixed mode in room B. We have shown that the attenuation index falls as  $\omega_0^{-1}$ , while the attenuation index for any fixed Fabry–Perot modes falls as  $\omega_0^{-3/2}$ .

We have formulated diffraction problems important for constructing the field in rectangular rooms.

## ACKNOWLEDGMENTS

This study was supported by the Russian Foundation for Basic Research (project no. 07-02-00803) and the program Scientific Schools.

## REFERENCES

1. H. Kutruff, *Room Acoustics* (Spon Press, New York, 2000).
2. Yu. I. Bobrovnikov, *Akust. Zh.* **50**, 751 (2004) [*Acoust. Phys.* **50**, 647 (2004)].
3. C. A. Brebbia, J. C. F. Telles, and L. C. Wrobel, *Boundary Element Techniques: Theory and Applications in Engineering* (Springer, Berlin, 1984; Mir, Moscow, 1987).
4. V. M. Babich and V. S. Buldyrev, *Asymptotic Methods in Short Wave Diffraction Problems* (Nauka, Moscow, 1972) [in Russian].
5. L. A. Vainshtein, *Open Resonators and Open Waveguides* (Sov. Radio, Moscow, 1966) [in Russian].
6. E. F. Ishchenko, *Open Optical Resonators* (Sov. Radio, Moscow, 1980) [in Russian].
7. Yu. A. Anan'ev, *Optical Resonators and the Beam Divergence Problem* (Nauka, Moscow, 1990) [in Russian].
8. V. V. Zalipaev, *J. Math. Sci.* **57**, 3101 (1991).
9. A. V. Shanin, *J. Appl. Math.* **70**, 1201 (2009).
10. B. Noble, *Methods Based on the Wiener–Hopf Technique* (Pergamon, Oxford, 1958; Fizmatlit, Moscow, 1962).
11. V. V. Zalipaev, *Zap. Nauch. Sem. POMI* **250**, 109 (1998).
12. V. V. Zalipaev and M. M. Popov, *Zap. Nauch. Sem. LOMI* **165**, 59 (1987).
13. V. V. Zalipaev and M. M. Popov, *Zap. Nauch. Sem. LOMI* **173**, 60 (1988).

*Translated by A. Carpenter*